Stable structures with high topological charge in nonlinear photonic quasicrystals

K. J. H. Law,[1] Avadh Saxena,[2] P. G. Kevrekidis,[3] and A. R. Bishop[2]

[1] *Warwick Mathematics Institute, University of Warwick, Coventry CV4 7AL, UK*
[2] *Theoretical Division and Center for Nonlinear Studies, Los Alamos National Laboratory, Los Alamos, NM 87545, USA*
[3] *Department of Mathematics and Statistics, University of Massachusetts, Amherst MA 01003-4515, USA*

Stable vortices with topological charge of 3 and 4 are examined numerically and analytically in photonic quasicrystals created by interference of 5 as well as 8 beams, in the cases of cubic as well as saturable nonlinearities . These structures are experimentally realizable, including a prototypical example of a stable charge 4 vortex. Direct numerical simulations corroborate the analytical and numerical linear stability analysis predictions.

PACS numbers: 42.65.Tg, 03.75.Lm, 61.44.Br, 63.20.Pw

Introduction. The study of coherent structures with non-vanishing topological charge has been a principal theme of interest in dispersive nonlinear systems with a wide range of applications including, among others, Bose-Einstein condensates (BEC) in atomic physics, and nonlinear optical media [1–4]. More recently, the study of such states has come to be of interest in settings with some discrete spatial symmetry i.e., nonlinear lattices. It was in this context that the notion of "discrete vortices" [5] arose and was subsequently intensely studied in both discrete and quasi-continuum media; see e.g. [6, 7] for relevant reviews. This, in turn, led to the experimental realization of unit-charge ($S = 1$) coherent structures in saturably nonlinear photorefractive media [such as SBN:75($Sr_0.75Ba_0.25Nb_2O_6$)] in [10, 11], as well as the exploration of higher charge ($S = 2$) ones in square as well as hexagonal/honeycomb lattice settings [8]. A multipole soliton necklace of out-of-phase neighboring lobes in a square lattice was identified experimentally and theoretically in [9] from initial condition of a wide $S = 4$ gaussian beam.

While such regular lattices have been a focal point of numerous studies [6], more recently experimental developments have enabled the study of photonic quasicrystals in photorefractive media [12], and have spurred a correspondingly intense theoretical activity [13]. We also note that recent experimental activity has focused on non-square optical lattices for ultracold atoms in the BEC case [14]. It is then natural to expect that quasi-crystals are well within experimental reach in this regard, as well.

Motivated by these developments, we illustrate the unique ability of such lattices (with saturable, but also with cubic nonlinearity) to sustain stable vortices of higher topological charge, such as $S = 3$ and $S = 4$. We illustrate the robustness of such modes, by means of direct numerical simulations. On the other hand, perhaps counter-intuitively (but as can be analytically predicted), modes with lower topological charge are found to be unstable, and this instability is also dynamically monitored. As we indicated, such modes should be directly accessible to present experiments in photorefractive media (and also, in principle, accessible in ultracold physics).

Theoretical Setup. We introduce the following non-dimensionalized evolution equation:

$$\left[i\partial_z + \frac{1}{2}\nabla^2 + F(|U|^2) - V(\mathbf{x})\right] U = 0. \tag{1}$$

In the motivating example of a photorefractive crystal, we have $F(|U|^2) = -1/(1 + |U|^2) + 1$, where U is the slowly varying amplitude of a probe beam normalized by the dark irradiance of the crystal I_d [4, 15], and V represents modulation of the refractive index from interfering linearly propagating waves normal to the probe beam, hence referred to as a photonic lattice. In the case of a Kerr medium the nonlinearity reads $F(|U|^2) = |U|^2$, and this case also includes the interpretation of U as a mean-field wavefunction of an atomic Bose-Einstein condensate [16] with the nonlinearity representing two-body contact interactions, while the potential V is either modulation of the refractive index in the former case or an externally applied field in the latter.

The potential V is taken to be of the form $E/(1+I(x))$, where $I(\mathbf{x}) = \frac{1}{N^2}\left|\sum_{j=1}^{N} e^{ik\mathbf{b}_j\cdot\mathbf{x}}\right|^2$. In the motivating case of a photorefractive crystal, this is the optical lattice intensity function formed by N interfering beams in the principal directions $\mathbf{b}_j$ with periodicity $2\pi/k$. We will consider the cases of $N = 5$ and $N = 8$. Here 1 is the lattice peak intensity, z is the propagation constant, $\mathbf{x} = (x, y)$ are transverse distances, $k = 2\pi/5$ is the wavenumber of the lattice, and $E = 5$ is proportional to the external voltage. Recently, such a setting has been explored theoretically for positive lattice solitons [13, 17], but we extend the considerations here to solutions of non-trivial topological charge.

The possible charge, S, of vortices (the number of 2π phase shifts across a discrete contour comprising the solution) is bounded by the symmetry of the lattice [18]. A lattice with n-fold symmetry has natural contours of $2n$ sites. Hence, taking into account the degeneracy of vortex anti-vortex pairs $\{S, -S\}$, one has $0 \le S \le n$,

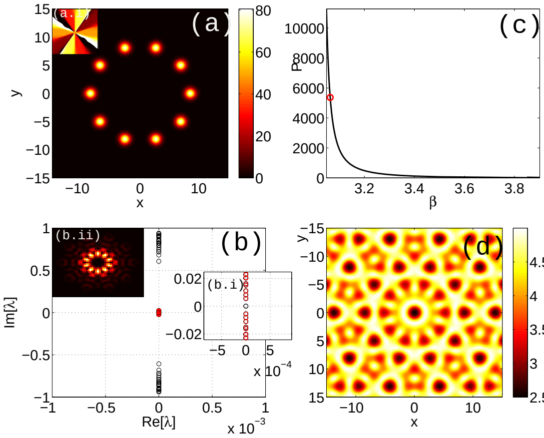

FIG. 1. (Color online) The stable $S = 4$ vortex in a quasi-crystal lattice of $N = 5$ and with a saturable nonlinearity. The profile and phase are depicted in panels [a(.i)], the linear spectrum in panel (b), Fourier spectrum in the inset panel (b.i), and continuation of the power, $P = \int |U|^2 d\mathbf{x}$, as a function of the propagation constant, β, in panel (c). The $N = 5$ lattice is depicted in (d).

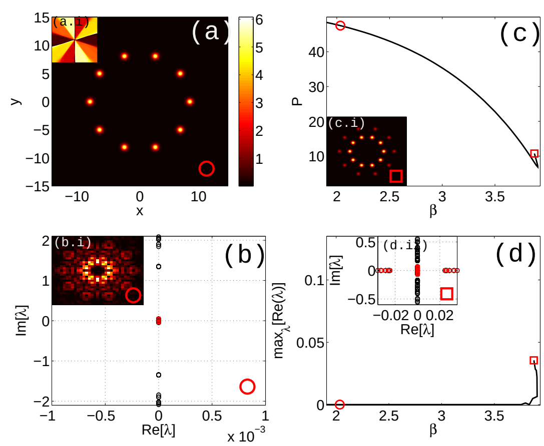

FIG. 2. (Color online) Panels (a-c) are the same as Fig. 1 except for a cubic nonlinearity. Panel (d) shows the growth rate, or $\max_\lambda[Re(\lambda)]$. The insets, (c.i) and (d.i) depict the profile and linear spectra, respectively, of the highly unstable solution indicated by a red square on the branches in (c,d), which collides with the main branch and disappears in a saddle node bifurcation close to the phonon band edge.

with the cases of $S = 0, n$ being the trivial flux cases of in-phase and out-of-phase neighboring lobes, respectively. The quasi-crystal with $N = 5$ has $n = 5$, while for $N = 8$, $n = 4$. Hence, the highest possible charge, $S = n - 1$, is $S = 4$ for the case of $N = 5$ and $S = 3$ for $N = 8$.

Considering the quasi-one-dimensional contour of excited sites (depending on the respective amplitudes of the lattice and the probe field), and within the context of coupled mode theory [19] in which the probe field is expanded in Wannier functions [20], one can obtain insights about the stability of the vortices within the framework of a discrete Nonlinear Schrödinger equation [7], $i\dot{u}_n = -\varepsilon(u_{n+1} + u_{n-1} - 2u_n) - |u_n|^2 u_n$. In that context and based on either the modulational instability of [19], or through empirical numerical testing [18] or, more rigorously, via Lyapunov-Schmidt perturbative expansions around the so-called *anti-continuum* (AC) limit of zero coupling ($\varepsilon = 0$) [21], it is known that lobes which are phase-separated by greater than $\pi/2$ are stable next to each other, while those separated by less than $\pi/2$ are unstable. A simple intuitive argument for this situation is that the effective potential which out-of-phase neighboring nodes exert on one another through the focusing non-linearity is one in which they repel each other, and, hence, remain localized in their respective separate wells. On the other hand, if the neighbors are in-phase, then the effective neighboring potentials are attractive to one another and hence the solution is unstable to remaining localized in separate wells. The possible relative phases interpolate between these cases, with $\pi/2$ being exactly in the middle. This leads to stability of the *higher* charged vortices for contours of larger numbers of nodes (see also [8]). We briefly review the Lyapunov-Schmidt argument. In the limit $\varepsilon \to 0$ one can construct exact solutions of the form $u_j = \sqrt{\mu} e^{\{-i(\beta t - \theta_j)\}}$ for any arbitrary $\theta_j \in [0, 2\pi)$ [21]. The case we are considering is that of $\theta_j = jS\pi/n$. We linearize around the solution for $\varepsilon = 0$ and the condition for existence of solutions with $\varepsilon > 0$ reduces to the vanishing of a vector function $\mathbf{g}(\boldsymbol{\theta})$ of the phase vector $\boldsymbol{\theta} = (\theta_1, \ldots, \theta_N)$, where

$$g_j \equiv \sin(\theta_{j-1} - \theta_j) + \sin(\theta_{j+1} - \theta_j), \qquad (2)$$

subject to periodic boundary conditions. This includes the discrete reduction of the vortex solutions for $0 \leq S \leq n$ above. The fundamental contours M will have length $|M| = 2n$, and $|\phi_{j+1} - \phi_j| = \Delta\phi = \pi S/n$ is constant for all $j \in M$, $|\theta_1 - \theta_{|M|}| = \Delta\theta$ and $\Delta\theta|M| = 0 \mod 2\pi$.

For the contour M, there are $|M|$ eigenvalues γ_j of the $|M| \times |M|$ Jacobian $\mathcal{M}_{jk} = \partial g_j/\partial\theta_k$ of the diffeomorphism given in Eq. (2). The eigenvalues of this matrix can be mapped to eigenvalues of the Hessian of the energy, which in turn can be mapped to the eigenvalues of the full linearization. In particular, eigenvalues of the linearization, denoted λ_j, are given to leading order by the relation [21] $\lambda_j = \pm\sqrt{2\gamma_j\varepsilon}$. Thus, solutions are stable to leading order if $\gamma_j < 0$ (so $\lambda_j \in i\mathbb{R}$) and unstable if $\gamma_j > 0$ (so $\lambda_j \in \mathbb{R}$). We have $\gamma_j = 4\cos(\Delta\phi)\sin^2\left(\frac{\pi j}{|M|}\right)$ and so these cases correspond exactly to the cases $\Delta\phi > \pi/2$ (or $S > n/2$) and $\Delta\phi < \pi/2$ (or $S < n/2$). In the boundary case of $\Delta\phi = \pi/2$, one needs to expand to the next order in the Lyapunov-Schmidt reduction. We note that a so-called staggering transformation along the contour, $u_j^d = (-1)^j u_j^f$ allows the conclusions for the focusing problem considered here to be mapped immediately to the analogous defocusing problem (with a change in the sign of the nonlinearity). We do not consider the defocusing case here, since the lowest allowable energies in this case occur for energies larger than the minimum energy of the linear spectrum, which has a fractal structure in the case of quasicrystals, rather than well-defined bands as in the case of a periodic lattice, and therefore cannot be resolved numerically as accurately. The above considerations illustrate the expectation that $S = 3$ vortices may be stable in the $N = 5$ and $N = 8$ cases, and the $S = 4$ vortex may be stable in the $N = 5$ case.

Numerical Results. We now turn to numerical computations to confirm the above expectations. We also explore the evolution of an $S = 4$ radial gaussian beam, which forms the expected stable structure, and find that in the case of cubic nonlinearity, the evolution sensitively depends on the particular perturbation.

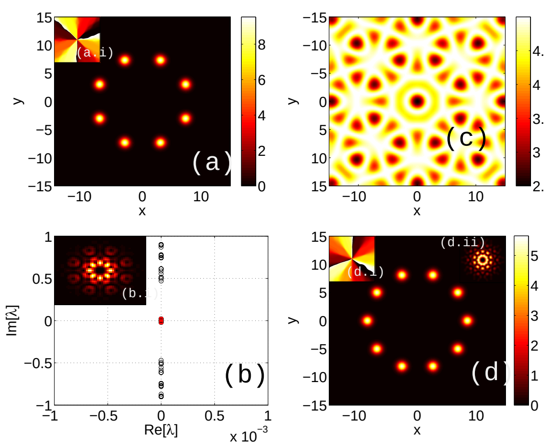

FIG. 3. (Color online) Panels (a,b) are the same as the previous figures for the stable $S = 3$ vortex in the $N = 8$ quasicrystal lattice (c). Panel (d) is the $S = 3$ vortex for $N = 5$ and [d.(i,ii)] are the phase and Fourier spectrum, respectively, of this solution. For both solutions, $\beta = 3.4$.

First, we confirm the expectation of stability of the $S = 4$ vortex for both saturable and cubic nonlinearities, over continuations in the semi-infinite gap (see Figs. 1 and 2, respectively). The profiles and phases are depicted in panels [a(.i)], linear spectra in panels (b), Fourier spectra in the inset panels (b.i), and continuations of the power, $P = \int |U|^2 d\mathbf{x}$, as a function of the propagation constant, β, in panels (c). It is notable that the power of the solution branches differs substantially between nonlinearities, and the power of the branch of saturable solutions approaches some resonant frequency at which $dP/d\beta \to \infty$ and $P \to \infty$ (see Fig. 1 (c)). The lattice is depicted in Fig. 1 (d), while Fig. 2 (d) shows the maximal perturbation growth rate, or $\max_\lambda[Re(\lambda)]$, corresponding to the branches in Fig. 2 (c).

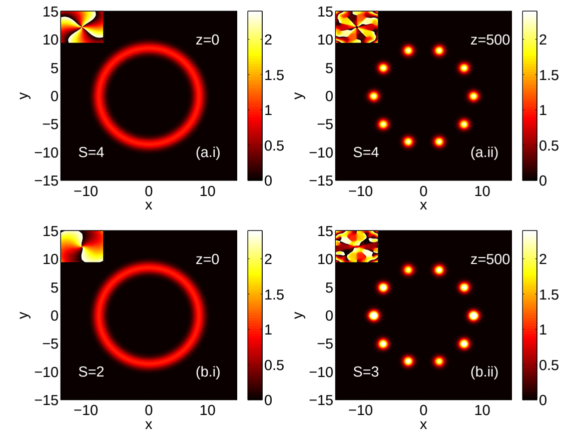

FIG. 4. (Color online) Initial conditions (a.i,b.i) and profiles at a later time (a.ii,b.ii) of the $S = 4$ and $S = 2$ radial Gaussian initial conditions for a saturable nonlinearity.

For the structures we consider, there is one pair of eigenvalues at the origin accounting for the U(1) (phase) invariance and the other $2n - 1$ eigenvalue pairs associated to the excited lobes all have negative energy, hence being candidates for instability [22], and are all either purely imaginary or purely real. If real, the instability is immediate, while if imaginary, instability may still arise due to their collision with the phonon band, or continuous spectrum, resulting in a Hamiltonian-Hopf bifurcation and a quartet of eigenvalues. The spectral plane, with the negative energy modes indicated by red squares, for the saturable and cubic cases are given in panels (b) of Figs. 1 and 2, respectively. Panel (b.ii) in Fig. 1 is a closeup of the origin showing the 9 negative energy pairs close to the origin and the one pair at the origin. The potential instability arising from these negative energy modes is prevented by their proximity to the origin, and being separated from the phonon energies. The expected saddle-node bifurcation [23, 24] occurs close to the band edge (which we computed as ≈ 3.9) in which the main solution collides (and disappears) with a solution branch of a configuration with additional populated sites external to the original contour and in-phase with those of the contour, resulting in instability due to real eigenvalues.

Next, we present results of the $S = 3$ vortex in both the $N = 8$ (Fig. 3(a,b)) and $N = 5$ (Fig. 3 (d)) cases for $\beta = 3.4$. Panel (c) depicts the $N = 8$ lattice, and [d.(i,ii)] are the phase and Fourier spectrum, respectively, of the solution in (d). These solutions are both stable, and again there is a resonance in the semi-infinite gap (not shown) similar to what was seen in Fig. 1. The vortices for $S < 3$ are unstable (not shown).

In order to examine the potential experimental realiz-

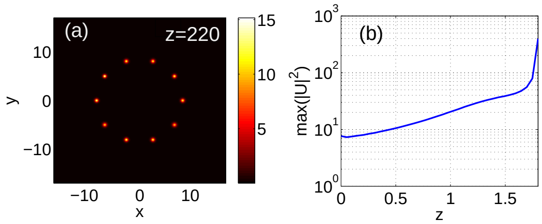

FIG. 5. (Color online) The dynamics of the unstable $S = 2$ vortex in the case of a cubic nonlinearity. Evolution of the same solution with the same perturbation of random noise with 5% of the initial maximum amplitude of the field can lead to robust structures that persist for long distances (a) and almost immediate collapse in different trials (b).

ability of the above waveforms, we launch a radial Gaussian beam with topological charge $S = 4$ of the form $e^{iS\theta-(r-R)^2/(2b^2)}$ with (r, θ) denoting polar coordinates, and $R = 8.5$, approximately the radius of the contour, and $b = 1$, as an initial condition into the system with saturable nonlinearity and monitor the evolution. After a transient period, the configuration indeed settles into an $S = 4$ vortex contour. For comparison, we launch a similar initial condition with $S = 2$ and notice it never settles into a stable configuration of fixed charge, although it does appear to maintain a relatively robust intensity distribution (i.e. 10 populated sites along the contour, although with fluctuating amplitudes). We introduce a relevant definition of topological charge within the contour of radius R in order to monitor its evolution

$$S = \frac{1}{2\pi} \oint \nabla\phi d\mathbf{r}, \tag{3}$$

where ϕ denotes the phase of the relevant complex field U.

See Fig. 4 for a presentation of the initial conditions (a.i,b.i) and profiles at a later time (a.ii,b.ii) of the $S = 4$ and $S = 2$ initial conditions, respectively, in a medium with saturable nonlinearity. The charge of each fluctuates, as power is shed and vortices nucleate in the surrounding low amplitude regions and enter and leave the contour as the solution finds the steady state. However, for the $S = 4$ initial condition, the field settles into a solution of constant charge 4, while for the $S = 2$ initial condition, the phase continues to fluctuate throughout the numerical experiment.

Finally, we examine the evolution of unstable ($S = 2$) vortices in the presence of a cubic nonlinearity. The evolution depends sensitively on the particular initial condition. In particular, using the initial condition $u = U(1 + X)$ with $X \sim 0.05\max_{\mathbf{x}}[U(\mathbf{x})]$ uniform[0,1], two different particular instances can lead to significantly different dynamics. In one instance, the phase merely reshapes as in the case of saturable nonlinearity, but the structure persists for a very long distance [see Fig. 5 (a)]. In another instance, the solution collapses almost immediately, as can be seen from the maximum amplitude of the field in Fig. 5 (b). For larger additive noise, collapse seems more likely from several sample trial simulations.

Conclusions and future directions. We have demonstrated numerically stable vortices of topological charge $S = 3$ in quasi-crystals with $n = 4$ and 5 directions of symmetry and $S = 4$ with $n = 5$, in the cases of both cubic as well as saturable focusing nonlinearities. The negative energy modes for these configurations remain close to the origin in the spectral plane, preventing collision with the phonon band, and hence there is a very good prospect for their experimental realization in photonic quasi-crystals in a photorefractive medium (or a Kerr medium). This has additionally been demonstrated by simulation of the evolution of a radial Gaussian beam into such robust vortex states. This is a prime prospect for an immediate future direction related to the present work. The evolution of the unstable $S = 2$ vortex in the case of a cubic nonlinearity depends sensitively on the particular perturbation, ranging from simple phase reshaping to almost immediate collapse.

Acknowledgements. KJHL gratefully acknowledges LANL and the CNLS for their hospitality during this research. This work was supported in part by the U.S. Department of Energy. PGK acknowledges NSF-DMS-0349023 and NSF-DMS-0806762.

[1] L.M. Pismen, *Vortices in Nonlinear Fields*, (Oxford University Press, Oxford, 1999).
[2] A.L. Fetter, Rev. Mod. Phys. **81**, 647 (2009).
[3] P.G. Kevrekidis *et al.*, Mod. Phys. Lett. B **18**, 1481 (2004).
[4] Y.S. Kivshar and G.P. Agrawal, *Optical Solitons: From Fibers To Photonic Crystals*, (Academic Press, London, 2003).
[5] B.A. Malomed and P.G. Kevrekidis, Phys. Rev. E **64**, 026601 (2001).
[6] F. Lederer *et al.*, Phys. Rep. **463**, 1 (2008).
[7] P.G. Kevrekidis, *The Discrete Nonlinear Schrödinger Equation*, (Springer-Verlag, Heidelberg, 2009).
[8] K.J.H. Law *et al.*, Phys. Rev. A **80**, 063817 (2009); B. Terhalle *et al.*, Phys. Rev. A **79**, 043821 (2009).
[9] J. Yang *et al.*, Phys. Rev. Lett. **94**, 113902 (2005).
[10] D.N. Neshev *et al.*, Phys. Rev. Lett. **92**, 123903 (2004).
[11] J.W. Fleischer *et al.*, Phys. Rev. Lett. **92**, 123904 (2004).
[12] B. Freedman, *et al.*, Nature **440**, 1166 (2006).
[13] M. J. Ablowitz, *et al.*, Phys. Rev. E **74**, 035601(R) (2006).
[14] C. Becker *et al.*, arXiv:0912.3646.
[15] N.K. Efremidis *et al.*, Phys. Rev. E **66**, 46602 (2002).
[16] L.P. Pitaevskii and S. Stringari, *Bose-Einstein Condensation*, (Oxford University Press, Oxford, 2003).
[17] Y. Sivan, *et al.*, Phys. Rev. E **78**, 046602 (2008).
[18] Y. V. Kartashov, *et al.*, Phys. Rev. Lett. **95**, 123902

(2005).
[19] D.N. Christodoulides and R.I. Joseph, Opt. Lett. **13**, 794 (1988); Yu.S. Kivshar and M. Peyrard, Phys. Rev. A **46**, 3198 (1992).
[20] W. Kohn, Phys. Rev. **115**, 809 (1959).
[21] D.E. Pelinovsky, P.G. Kevrekidis, and D.J. Frantzeskakis, Physica D **212**, 1 and 20 (2005).
[22] J. C. van der Meer, Nonlinearity **3**, 1041 (1990).
[23] J. Wang and J. Yang, Phys. Rev. A. **77**, 033834 (2008).
[24] H. Susanto *et al.*, Physica D **237**, 3123 (2008).